Received: 11 September 2020 | Revised: 5 February 2021 | Accepted: 15 February 2021

DOI: 10.1111/exd.14307

CONCISE COMMUNICATION

Experimental Dermatology WILEY

Inhibition of pyruvate oxidation as a versatile stimulator of the hair cycle in models of alopecia

Aimee Flores[1,2] | Sekyu Choi[3] | Ya-Chieh Hsu[3] | William E. Lowry[1,2,4,5,6]

[1]Department of Molecular Cell and Developmental Biology, UCLA, Los Angeles, CA, USA

[2]Pelage Pharmaceuticals, Inc., Los Angeles, CA, USA

[3]Department of Stem Cell and Regenerative Biology, Harvard University, Cambridge, MA, USA

[4]Division of Dermatology, David Geffen School of Medicine, UCLA, Los Angeles, CA, USA

[5]Molecular Biology Institute, UCLA, Los Angeles, CA, USA

[6]Broad Center for Regenerative Medicine, UCLA, Los Angeles, CA, USA

Correspondence
William E. Lowry, Department of Molecular Cell and Developmental Biology, UCLA, 621 Charles E. Young Drive South, Los Angeles, CA 90095, USA.
Email: blowry@ucla.edu

Funding information
National Institute of Arthritis and Musculoskeletal and Skin Diseases, Grant/Award Number: NIH 5R01AR070245-03; Pelage Pharmaceuticals, Inc., Grant/Award Number: 20184937

Abstract

Hair follicle stem cells (HFSCs) are known to be responsible for the initiation of a new hair cycle, but typically remain quiescent for very long periods. In alopecia, or hair loss disorders, follicles can be refractory to activation for years or even permanently. Alopecia can be triggered by autoimmunity, age, chemotherapeutic treatment, stress, disrupted circadian rhythm or other environmental insults. We previously showed that hair follicle stem cells and the hair cycle can be manipulated by regulation of pyruvate entry into mitochondria for subsequent oxidation to fuel the TCA cycle in normal adult mice with typical hair cycling. Here, we present new data from our efforts to develop murine models of alopecia based on environmental triggers that have been shown to do the same in human skin. We found that inhibition of pyruvate transport into mitochondria can accelerate the hair cycle even during refractory hair cycling due to age, repeated chemotherapeutic treatment and stress. Hair cycle acceleration in these alopecia models led to the formation of histologically normal hair follicles within 30–40 days of treatment without any overt signs of toxicity or deleterious effects. Therefore, we propose inhibition of pyruvate entry into mitochondria as a versatile treatment strategy for alopecia in humans.

KEYWORDS
alopecia, hair loss, metabolism, mitochondrial pyruvate carrier, MPC

1 | BACKGROUND

The hair cycle is known to proceed through various stages of rest (telogen), reactivation (anagen) and degradation (catagen).[1–3] The cycle is known to be regulated by a variety of factors both intrinsic and extrinsic, including signalling cascades, transcription factors, systemic stress and ageing. How these signals act on the hair follicle has been fleshed out over the last 40 years, and new players are recognized each year.[4] One target population for this regulatory scheme is hair follicle stem cells (HFSCs) in the bulge and hair germ.[3,5–8] These cells are known to lie dormant for long periods between hair cycles and activate at the start of a hair cycle.[9–11] They are known to be sensitive to stimulation by signalling cascades such as Wnt, FGF and BMP, and their quiescence is known to be maintained by transcription factors such as Nfatc, Foxc1 and Tcf3.[4,12–16] Recent work from our laboratory and others have shown that manipulation of cellular metabolism in hair follicle stem cells can regulate their activation and consequentially the hair cycle itself.[17–20] At the start of a new hair cycle, progenitor cells in the hair germ are the first to show signs of activation upon migration of hair follicle stem cells from the bulge into the hair germ.[8] Then, hair follicle stem cells in the bulge are replenished through self-renewal.[8] Therefore, the first sign of hair cycle activation (exit from telogen) is proliferation in the hair germ.

Previously, it was shown that human hair follicles in general use both aerobic glycolysis and glutaminolysis to power their

metabolism.[21–23] We used recombination with K15CrePR1 to show that murine hair follicle stem cells in the bulge and hair germ take more advantage of glucose uptake and generation to lactate than their epidermal counterparts.[18] We found that hair cycle activation happens coincident with increased lactate dehydrogenase activity in the bulge and that deletion of the enzyme responsible for this activity blocks the ability of bulge and hair germ cells to initiate a new hair cycle. Conversely, we showed that activation of Ldh activity by induction of Ldh enzyme production can stimulate the hair cycle. Finally, we showed that genetic or pharmacological inhibition of pyruvate entry into the mitochondria can increase Ldh activity and accelerate the hair cycle as well. Inhibition of pyruvate oxidation via blockade of the mitochondrial pyruvate carrier (MPC) complex is known by studies in several species and contexts to increase Ldh activity by providing more substrate for the enzyme to convert to lactate. UK5099 is a bona fide inhibitor of the MPC carrier complex and is known to block pyruvate from entering the mitochondrion, which then leads to increase conversion of pyruvate to lactate via the lactate dehydrogenase enzyme.[24–26] This is the same enzyme we previously showed was critical to hair cycle activation and initiation of the hair cycle.[18] In both mice and lower organisms, treatment of cells with UK5099 is known to effectively increase Ldh activity.[24,25,27,28]

We and others also showed that inhibition of the electron transport chain in the skin can also lead to stimulation of Ldh activity and activation of the hair cycle.[19,29,30] All these studies showed that increased Ldh activity or inhibition of the electron transport chain correlates with an accelerated hair cycle, but none of them determined whether direct inhibition of MPC could stimulate the hair growth in models of alopecia. With the development of UK5099 and analogues, it is possible that a simple topical compound could be used to treat hair loss, but first this must be shown to be feasible in authentic models of alopecia.

Therefore, we exploited existing knowledge of causes of alopecia and adapted them to determine whether MPC inhibition is a viable method to promote hair growth in response to a variety of deleterious stimuli. We took advantage of murine models of alopecia due to ageing, repeated rounds of chemotherapy and environmental stress.[31–37] Two of these models have been in use for decades (Ageing and Chemo), and a third has been appreciated, but not quantified until more recently (Stress). In each case, the alopecia appears in adult animals after shaving, where regions of the backskin show patches of bald skin that appear to persist for at least months in some cases, or permanently in others. In most cases, little is known about how to reverse this refractory telogen, with the exception of minoxidil, a popular pharmaceutical.[33] In each case, inhibition of MPC was able to accelerate the hair cycle without causing deleterious effects, presumably by restoring hair follicle stem and progenitor cells (bulge and hair germ) activation in follicles that had become refractory to activation.

2 | EXPERIMENTAL DESIGN

2.1 | Age-induced alopecia

Like humans, ageing mice show altered regenerative hair capacity. Although hair follicles in ageing skin retain their stem cell compartments, they cycle more slowly and remain in prolonged telogen. Several studies have shown that this deterioration in regenerative ability can be due to signalling defects intrinsic to stem cells, the niche or both.[38,39] Age-associated changes in the extra-niche macroenvironment has also been shown to play a key role in modulating hair follicle regeneration.[38–41] As in humans, ageing in mice leads to the greying and thinning of hair.[42–44] The presence of hair follicle stem cells in aged skin potentially provides an avenue to restart the hair cycle. In previous studies, MPC inhibition was sufficient to accelerate a transition from telogen to anagen in adult animals earlier than normal. However, we did not show that this would also work in aged animals, where follicles are refractory to initiation of anagen. Shaving mice that were at least 18 months of age routinely yielded backskin with patchy fur, with some regions appearing to be completely resistant to anagen initiation over weeks to months. Ageing in these mice prior to treatment was also obvious from simple observation as the skin was flaky, wrinkled and drier than in young mice (Figure 1A). Complete methods are provided in Appendix S1.

2.2 | Chemotherapy-induced alopecia

Next, we attempted to develop a model of chemotherapy-induced alopecia. A fraction of all people taking cytotoxic chemotherapies

FIGURE 1 Pharmacological inhibition of Mpc1 promotes hair cycle activation in Ageing Mice. (A) Animals treated topically with UK-5099 (20 μM) show pigmentation and hair growth, indicative of entry into anagen, after 12 days of treatment. Full anagen, indicated by full coat of hair, is achieved after 30 days of treatment. Mice treated topically with vehicle control show less pigmentation and hair growth at both Day 12 and Day 30. (B) Graph showing the average percent hair coverage after 30 days of topical treatment with UK-5099 (20 μM) or Vehicle. n = 12 mice per condition. Shown as mean ± SEM. Paired t test was performed, $p < 0.05$. (C) Graph showing no difference in the average number of follicles between Vehicle and UK-5099 (20 μM)-treated mice, but differences in average number of follicles in telogen, transition and anagen, right graph. n = 8 mice per condition. Shown as mean ± SEM. Paired t test was performed, $p < 0.05$. (D) Skin pathology showing that UK-5099-treated animals have more follicles in anagen at Day 30 typified by down growth of the follicle and hypodermal thickening, while vehicle control-treated animals show more follicles remained in telogen. Images shown are representative of at least 8 mice from 3 independent experiments. Scale bars indicate 100 micrometres. (E) Immunofluorescence staining for proliferation (Ki67) in HFSCs (Sox9) showing increased proliferation of hair germ cells in UK-5099-treated animals after 30 days of topical treatment. Images shown are representative of at least 8 mice from 3 independent experiments. Scale bars indicate 50 micrometres. (F) Quantification of Ki67-positive cells in hair follicle bulge and hair germ of Vehicle and UK5099-treated aged mice. n = 12 follicles per condition. Shown as mean ± SEM

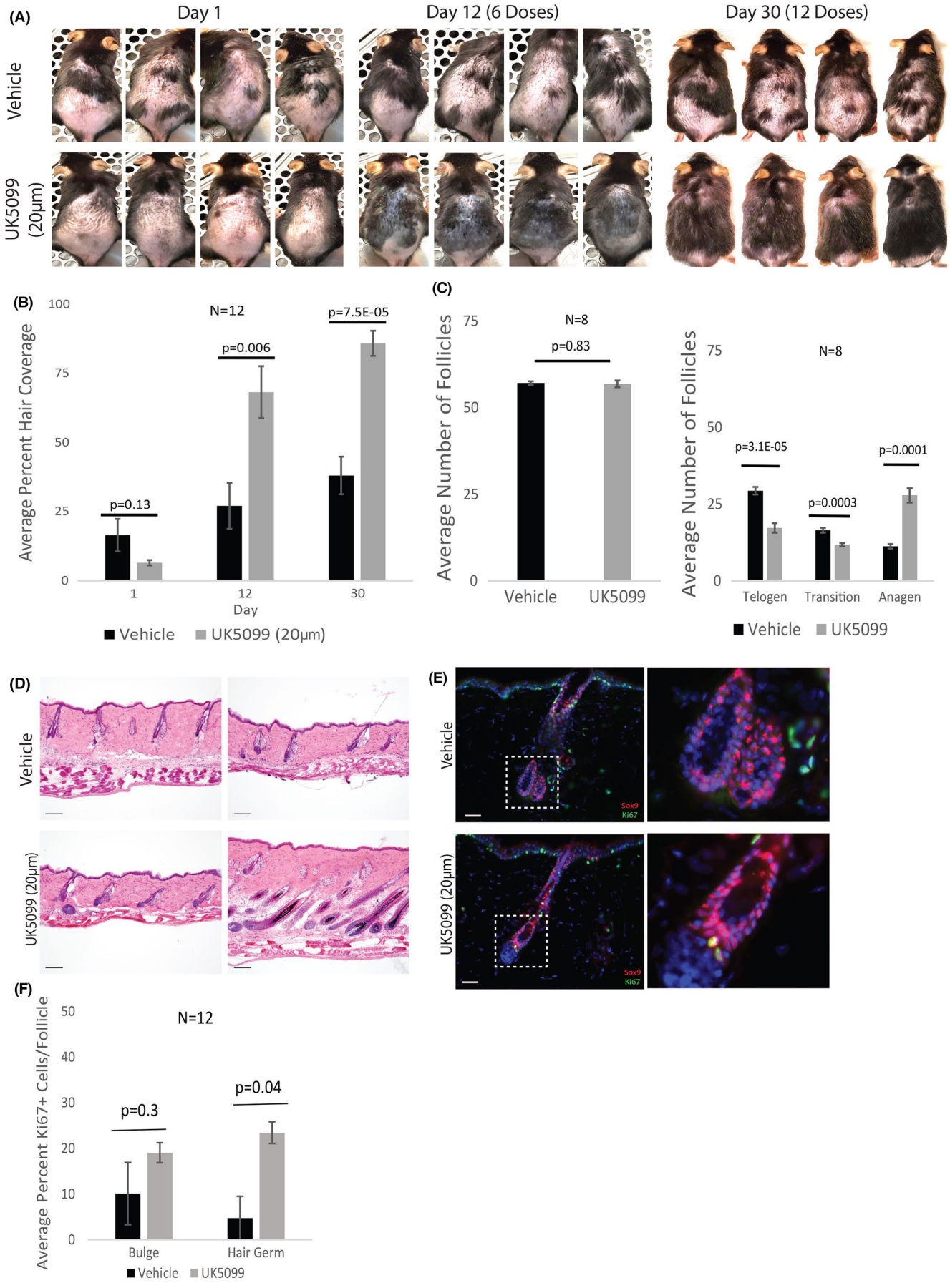
(A)
Day 1
Day 12 (6 Doses)
Day 30 (12 Doses)
Vehicle
UK5099 (20μm)
(B)
Average Percent Hair Coverage
N=12
p=0.006
p=7.5E-05
p=0.13
Day
Vehicle
UK5099 (20μm)
(C)
Average Number of Follicles
N=8
p=0.83
Vehicle
UK5099
N=8
p=3.1E-05
p=0.0003
p=0.0001
Telogen
Transition
Anagen
Vehicle
UK5099
(D)
Vehicle
UK5099 (20μm)
(E)
Vehicle
UK5099 (20μm)
Sox9
Ki67
(F)
Average Percent Ki67+ Cells/Follicle
N=12
p=0.3
p=0.04
Bulge
Hair Germ
Vehicle
UK5099

experience permanent hair loss.[45–48] These patients suffer from alopecia even though their follicles are intact,[45,46] because the follicles appear to be stuck in telogen. Cyclophosphamide-induced alopecia in C57BL/6J mice captures key features of the chemotherapy-induced hair loss that is seen in patients with cancer and has been shown to be a clinically relevant model for studying the biology of chemotherapy-induced hair loss in humans.[31,49,50] Chemotherapy-induced damage and recovery patterns of hair depend on various factors including dosage, type of chemotherapeutic agent and treatment schedule. While chemotherapy-induced alopecia is usually reversible, permanent hair loss can occur in patients treated with repetitive high-dose chemotherapeutic agents, and additional studies are needed to study the effects of multiple treatments of chemotherapeutic agents specifically on hair follicles.[31,51–54] To mimic this situation in a murine model, we treated mice with multiple rounds of the chemotherapeutic cyclophosphamide.[46,55] After each round of treatment, the mice lost their hair, and then the hair regrew (Figure 2A). However, after 6–8 rounds of chemotherapy and hair cycling, the hair coat came back in thinner, the result of fewer follicles re-entering anagen (Figure 2A), consistent with what is observed in some patients taking chemotherapies.

2.3 | Alopecia due to chronic stress

Chronic stress is also known to induce reversible alopecia. In vivo and in vitro mouse models have demonstrated that chronic stress is significantly associated with hair loss, and the presence of stress-mediating substances such as cortisol, prolactin and substance P can inhibit hair growth.[33,56–59] A new understanding of this phenomena was recently described to be due to sympathetic nerve innervation directly on hair follicle stem cells.[60–63] In murine models of stress (circadian, auditory, ambulatory),[64] it was shown that shaving mice during adult telogen leaves animals without hair for an extended period (Hsu et al, in revision) through corticosterone signalling. Different strains of mice react differently to various methods of stress application, and C57BL/6 mice have been shown to be particularly sensitive to most stressors. In this study, C57BL/6 mice were exposed to chronic socioenvironmental stressors for several weeks.[64] We used this model to determine whether MPC inhibition could overcome stress-induced alopecia. First, we modelled stress by subjecting mice to various noxious stimuli as described in [64]and Hsu et al., in review,[65] and found that after shaving the backskin, hair did not grow back for an extended period (Figure 3A).

3 | RESULTS

We treated aged mice with either Vehicle (Transderma PLO gel or Neutrogena lotion) or Vehicle +UK5099 (20 μM). Treatment is topical, with 200 microliters of formulation applied every other day onto shaved skin. We then observe hair regrowth and chronicle the hair cycle by taking photographs and quantifying pigmentation and then the emergence of hair. Aged mice treated with UK5099 grew back hair with greater coverage than vehicle alone, suggesting that this drug was activating dormant follicles. UK5099 increased the coverage area of hair by roughly twofold (Figure 1B) macroscopically. After 30 days of treatment, tissue was harvested, and microscopic analysis showed increased percentage of follicles entering anagen, without affecting the number of follicles in total (Figure 1C). The evidence points to a reactivation of dormant follicles by UK5099, as shown by the ratio of follicles in telogen versus anagen (Figure 1C). The histology of the skin in both vehicle and UK5099-treated conditions was similar with no overt differences except for hair follicles in anagen (Figure 1D). Furthermore, immunostaining for markers of proliferation and hair follicle stem cells showed that the first response to MPC inhibition was proliferation in the hair germ, as expected in the two-step model described above (Figure 1E).

We next shaved mice undergoing the chemotherapy paradigm and then treated with vehicle or UK5099 to see whether blocking pyruvate oxidation could promote reactivation of dormant follicles. We harvested tissue from these animals once the macroscopic phenotype became apparent, which was typically 30 days after treatment began. Treatment of mice with UK5099 led to increased hair growth versus vehicle in much the same way it did in aged mice (Figure 2B-D). This happened without new hair follicles being formed, nor with any

FIGURE 2 Pharmacological inhibition of Mpc1 promotes hair cycle activation in Chemotherapy-treated mice. (A) Wild-type C57BL/6J mice treated intraperitoneally with multiple rounds of low dose (120 mg/kg) chemotherapeutic cyclophosphamide. Mice lost and regrew their hair thinner after each round. After 8 rounds of chemotherapy little to no hair growth was observed. (B) Animals treated topically with UK-5099 (20 μM) show pigmentation and hair growth, indicative of entry into anagen, after 14 days of treatment. Full anagen, indicated by full coat of hair, is achieved after 30 days of treatment. Mice treated topically with vehicle control show less pigmentation and hair growth at both Day 12 and Day 30. (C) Graph showing greater average percent hair coverage after 30 days of topical treatment with UK-5099 (20 μM) compared with Vehicle. n = 12 mice per condition. Shown as mean ± SEM. Paired t test was performed, $p < 0.05$. (D) Graph showing no difference in the average number of follicles between Vehicle and UK-5099 (20 μM)-treated mice, but differences in average number of follicles in telogen, transition and anagen, right graph. n = 12 mice per condition. Shown as mean ± SEM. Paired t test was performed, $p < 0.05$. (E) Skin pathology showing that UK-5099-treated animals have more follicles in anagen at Day 30 typified by down growth of the follicle and hypodermal thickening, while vehicle control-treated animals show more follicles remained in telogen. Images shown are representative of at least 12 mice from 3 independent experiments. Scale bars indicate 100 micrometres. (F) Immunofluorescence staining for proliferation (Ki67) in HFSCs (Sox9) showing increased proliferation of stem cells in UK-5099-treated animals after 30 days of topical treatment. Images shown are representative of at least 12 mice from 3 independent experiments. Scale bars indicate 50 micrometres. (G) Quantification of Ki67-positive cells in hair follicle bulge and hair germ of Vehicle and UK5099-treated mice following chemotherapy. n = 12 follicles per condition. Shown as mean ± SEM

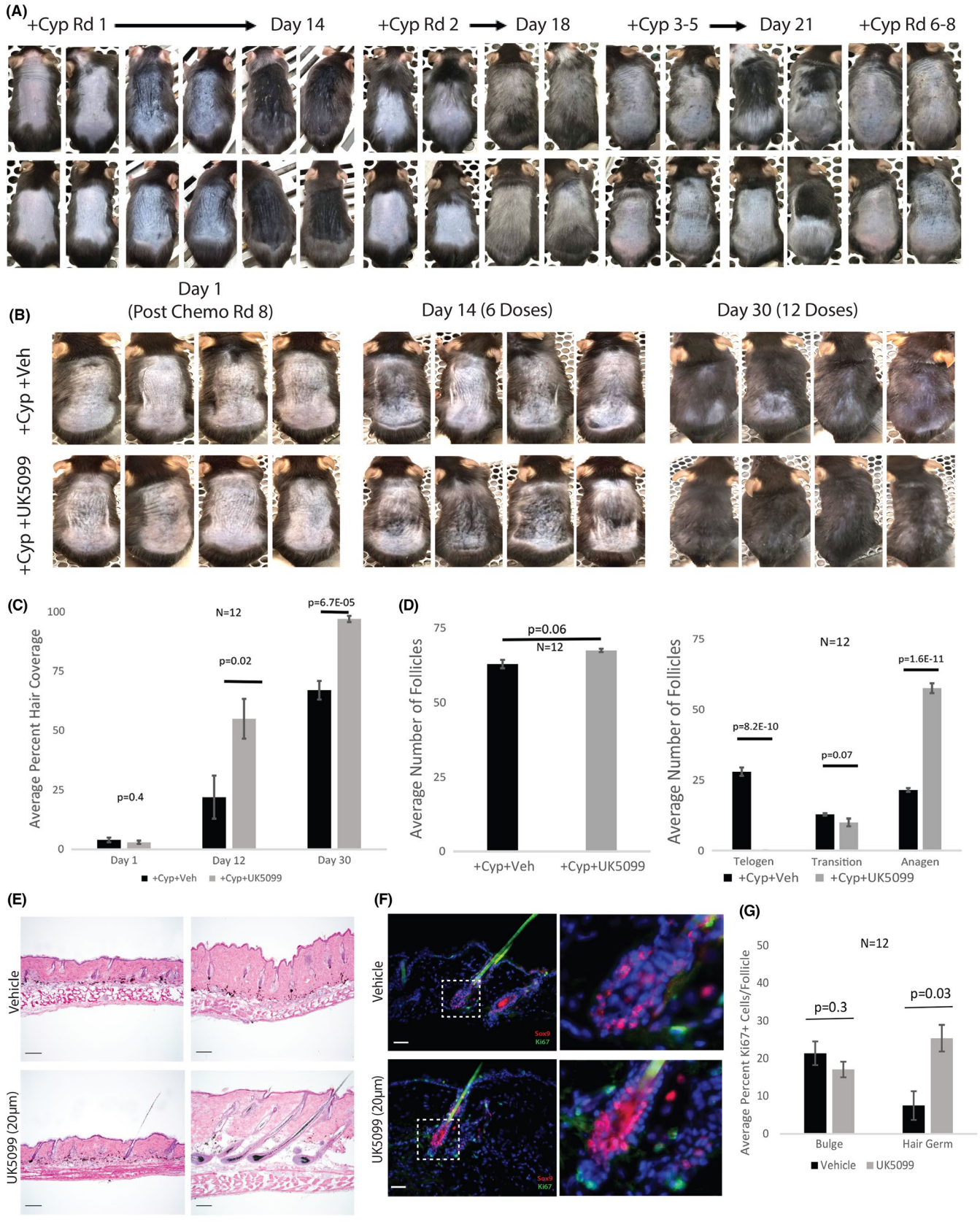

dramatic alterations to normal hair morphology, as judged by histology and staining for markers of various cell types within the follicle (Figure 2E,F). Together, these data appear to be consistent with the effect of MPC inhibition observed in ageing mice; the treatment with MPC inhibitor led to an activation of refractory hair germs, and an increased number of follicles entering anagen (Figure 2).

Finally, in animals undergoing the chronic stress paradigm, we also found that topical application of UK5099 drove an acceleration

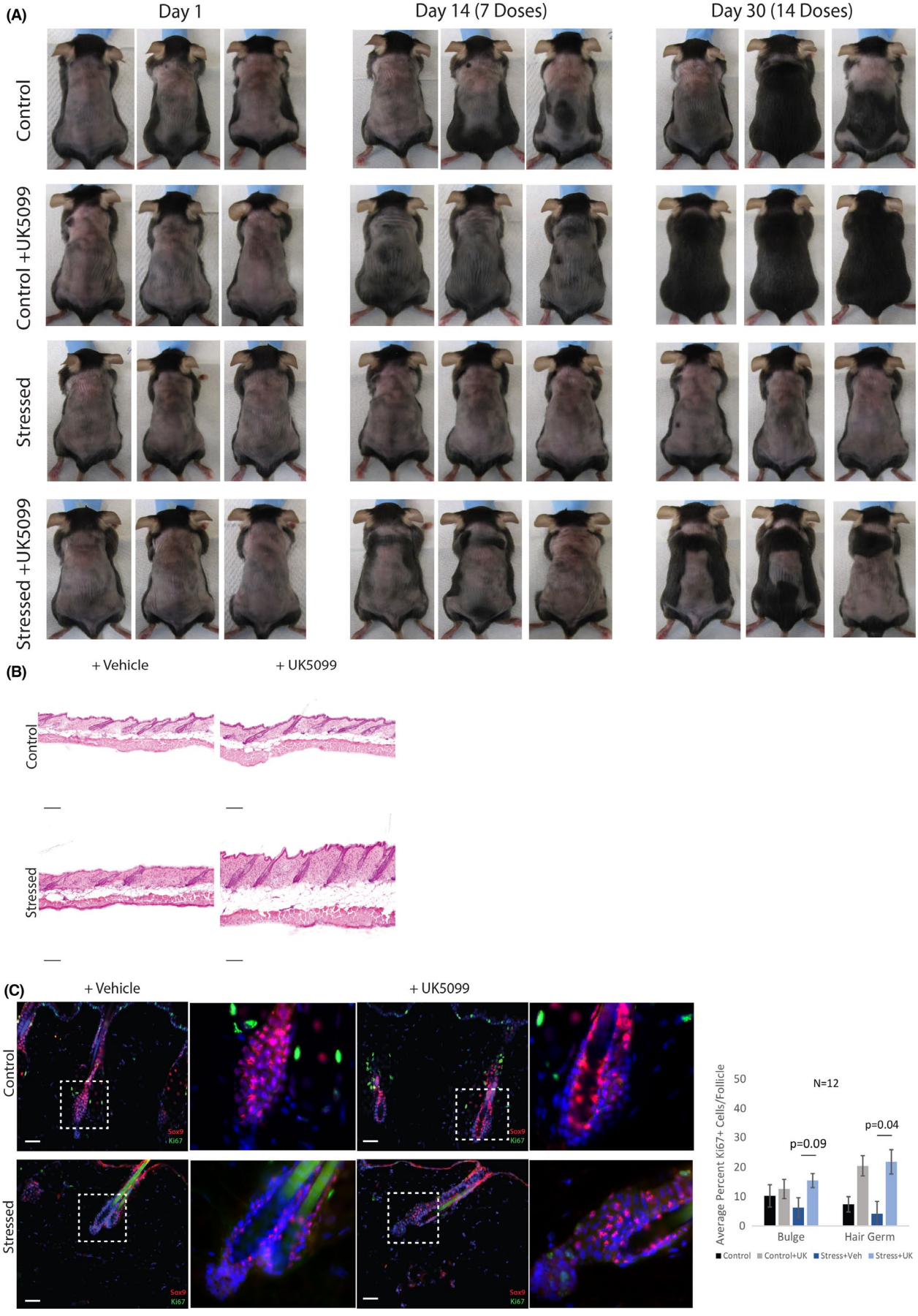

FIGURE 3 (Continued)

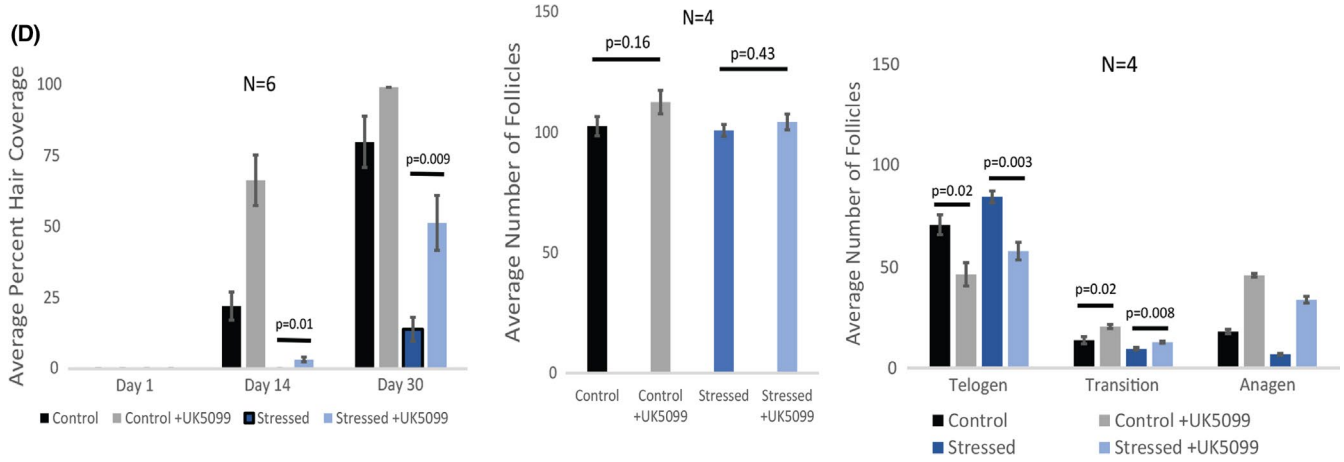

FIGURE 3 Pharmacological inhibition of Mpc1 promotes hair cycle activation in Stressed Mice. (A) Both control and stressed animals treated topically with UK-5099 (20 μM) show pigmentation and hair growth, indicative of entry into anagen, after 14 days of treatment. Full anagen, indicated by full coat of hair, is achieved after 30 days of treatment. Control mice treated topically with Vehicle show less pigmentation and hair growth at both Day 12 and Day 30. Stressed mice treated topically with Vehicle show no hair growth and only minimal pigmentation even after 30 days. (B) Skin pathology showing that UK-5099-treated animals have more follicles in transition at Day 30 while vehicle control treated, and stressed animals show more follicles remained in telogen. Images shown are representative of at least 6 mice from 2 independent experiments. Scale bars indicate 100 micrometres. (C) Immunofluorescence staining for proliferation (Ki67) in HFSCs (Sox9) showing increased proliferation in UK-5099 treated animals after 30 days of topical treatment. Images shown are representative of at least 8 mice from 3 independent experiments. Scale bars indicate 50 micrometres. right graph Quantification of Ki67-positive cells in hair follicle bulge and hair germ of Vehicle and UK5099-treated mice following stress. n = 12 follicles per condition. Shown as mean ± SEM. (D) Graph showing greater average percent hair coverage after 30 days of topical treatment with UK-5099 (20 μM) compared with Vehicle. n = 6 mice per condition. Shown as mean ± SEM. Paired t test was performed, $p < 0.05$. right, Graph showing no difference in the average number of follicles between Control, Stressed, Vehicle and UK-5099 (20 μM)-treated mice, but differences in average number of follicles in telogen, transition and anagen, far right graph. n = 4 mice per condition. Shown as mean ± SEM. Paired t test was performed, $p < 0.05$

of hair follicle activation and growth in patches of the backskin (Figure 3A). Tissue was again harvested once the phenotype became apparent. Microscopic analysis demonstrated that application of UK5099 induced telogen to anagen transition without deleterious effects on the histology of the skin, or changes to numbers of hair follicle stem cells (Figure 3B-E).

Taken together, these data are consistent with the notion that several forms of alopecia can occur without permanent disruption of hair follicle stem cells and that MPC inhibition can be an effective method to promote activation of the hair cycle. The fact that MPC inhibition was successful at regulating the hair cycle in three different models of alopecia is consistent with the notion that pyruvate metabolism can be an important intrinsic regulator of hair follicle stem cell function.

4 | CONCLUSIONS AND PERSPECTIVES

Here, we found that MPC inhibition can promote an acceleration of the hair cycle in several models of alopecia where follicles are refractory to activation due to environmental stressors. Our previous studies demonstrated that MPC inhibition was sufficient to accelerate the typical adult hair cycle. Left unknown from these studies was whether MPC inhibition could activate follicles that are dormant due to various other stressors not assessed here. By further developing models of alopecia due to age, chemotherapy or stress, this study also opens avenues to more deeply understand the regulatory mechanisms driving hair follicle stem cell activation and the hair cycle.

This study also raises important questions for future studies. For instance, while MPC inhibition was able to overcome refractory hair cycles, we did not determine whether defects in metabolism are triggers for alopecia due to environmental or systemic insults. This type of study will require a systematic exploration of metabolomics with radiotracers on isolated cell types across different timepoints in the various models. Our previous studies with metabolomic analysis did not employ radio-tracing metabolites and sorting cell types due to technical limitations, but this is an active area of investigation.

In addition, this current work does not define specifically a role for MPC inactivation particularly in hair follicle stem cells in the bulge or hair germ. Our previous study used molecular genetics to target the Mpc1 deletion to the HFSC population using a K15CrePR promoter-driven strategy. This method directs recombination to both HFSCs in the bulge and the hair germ. We found that deletion of Mpc1 in the bulge and hair germ could affect the hair cycle, whereas deletion in other cell types of the follicle was unable to have an effect. Those data coupled with numerous studies over the years showing that HFSCs are critical for regulation of the hair cycle leads us to presume that the effects of MPC inhibition seen here were indeed acting on the bulge and hair germ. Here, we focused our efforts on showing the effect of MPC inhibition in the context of multiple models of alopecia, using a topical approach that inhibits MPC in all cell types of the epidermis and the follicle. Therefore, in this study,

we cannot say for certain that the effect seen was due to MPC inhibition strictly in the HFSCs.

It is tempting to speculate that MPC inhibition could be a potential clinical avenue to promote hair growth in a variety of settings, including those described here. Previous efforts to exploit metabolic manipulation to regulate the hair cycle focussed on just the normal cycle, not in settings where entry to anagen is refractory. Because the treatment is effective as a topical pharmaceutical, one could argue that there is a clear path to the clinic. However, to justify translation to the clinic, it is first essential to determine whether human bulge and hair germ cells are subject to the same type of unique metabolic pattern that has been found in murine follicles. Even if the pattern is conserved, there is no guarantee that MPC inhibition would promote the hair cycle in human follicles, where there appear to be numerous similarities and differences with murine follicles.[4,66] Regardless, it will be challenging to determine whether human follicles functionally respond to MPC inhibition in a similar fashion as murine follicles until clinical studies can be initiated.

ACKNOWLEDGMENTS

We would like to acknowledge those that made this work possible including the staff at DLAM, the animal facility at UCLA. Y-C. H. is a Pew Scholar and a New York Stem Cell Foundation—Robertson Investigator. This work was supported by both the National Institute of Arthritis and Musculoskeletal and Skin Diseases (NIH 5R01AR070245-03) and a Sponsored Research Agreement (Pelage Pharmaceuticals, 20184937) to WEL.

CONFLICT OF INTEREST

This work was supported by a Sponsored Research Agreement funded by Pelage Pharmaceuticals, which is attempting to develop pharmaceutical interventions for Alopecia. WEL is a founder and President of Pelage Pharmaceuticals, Inc. AAF is now a Senior Scientist at Pelage Pharmaceuticals.

AUTHOR CONTRIBUTIONS

AAF designed, collected and disseminated the data, and wrote the manuscript. SC and YCH designed and collected all the data on the chronic stress model. WEL wrote the manuscript.

DATA AVAILABILITY STATEMENT

The data in this manuscript will be made available upon request.

ORCID

Aimee Flores https://orcid.org/0000-0002-3112-8934
Sekyu Choi https://orcid.org/0000-0003-2928-0942
Ya-Chieh Hsu https://orcid.org/0000-0002-0178-7373
William E. Lowry https://orcid.org/0000-0003-2932-2276

REFERENCES

1. Alonso L, Fuchs E. The hair cycle. *J Cell Sci*. 2006;119:391-393.
2. Paus R, Foitzik K. In search of the "hair cycle clock": a guided tour. *Differentiation*. 2004;72:489-511.
3. Fuchs E, Merrill BJ, Jamora C, et al. At the roots of a never-ending cycle. *Dev Cell*. 2001;1:13-25.
4. Plikus MV. New activators and inhibitors in the hair cycle clock: targeting stem cells' state of competence. *J Invest Dermatol*. 2012;132:1321-1324.
5. Tumbar T, Guasch G, Greco V, et al. Defining the epithelial stem cell niche in skin. *Science*. 2004;303:359-363.
6. Lavker RM, Sun TT, Oshima H, et al. Hair follicle stem cells. *J Investig Dermatol Symp Proc*. 2003;8:28-38.
7. Lavker RM, Miller S, Wilson C, et al. Hair follicle stem cells: their location, role in hair cycle, and involvement in skin tumor formation. *J Invest Dermatol*. 1993;101:16S-26S.
8. Greco V, Chen T, Rendl M, et al. A two-step mechanism for stem cell activation during hair regeneration. *Cell Stem Cell*. 2009;4:155-169.
9. Watt FM, Jensen KB. Epidermal stem cell diversity and quiescence. *EMBO Mol Med*. 2009;1:260-267.
10. Nishikawa SI, Osawa M, Yonetani S, et al. Niche required for inducing quiescent stem cells. *Cold Spring Harb Symp Quant Biol*. 2008;73:67-71.
11. Cotsarelis G. Epithelial stem cells: a folliculocentric view. *J Invest Dermatol*. 2006;126:1459-1468.
12. Choi YS, Zhang Y, Xu M, et al. Distinct functions for Wnt/beta-catenin in hair follicle stem cell proliferation and survival and interfollicular epidermal homeostasis. *Cell Stem Cell*. 2013;13:720-733.
13. Oshimori N, Fuchs E. Paracrine TGF-beta signaling counterbalances BMP-mediated repression in hair follicle stem cell activation. *Cell Stem Cell*. 2012;10:63-75.
14. Nishimura EK, Suzuki M, Igras V, et al. Key roles for transforming growth factor beta in melanocyte stem cell maintenance. *Cell Stem Cell*. 2010;6:130-140.
15. Zhang J, He XC, Tong WG, et al. BMP signaling inhibits hair follicle anagen induction by restricting epithelial stem/progenitor cell activation and expansion. *Stem Cells*. 2006;24:2826-2839.
16. Millar SE, Willert K, Salinas PC, et al. WNT signaling in the control of hair growth and structure. *Dev Biol*. 1999;207:133-149.
17. Jelinek D, Flores A, Uebelhoer M, et al. Mapping metabolism: monitoring lactate dehydrogenase activity directly in tissue. *J Vis Exp*. 2018;136:57760.
18. Flores A, Schell J, Krall AS, et al. Lactate dehydrogenase activity drives hair follicle stem cell activation. *Nat Cell Biol*. 2017;19:1017-1026.
19. Miranda M, Christofk H, Jones DL, et al. Topical inhibition of the electron transport chain can stimulate the hair cycle. *J Invest Dermatol*. 2018;138:968-972.
20. Kim CS, Ding X, Allmeroth K, et al. Glutamine metabolism controls stem cell fate reversibility and long-term maintenance in the hair follicle. *Cell Metab*. 2020;32:629.e8-642.e8.
21. Kealey T, Williams R, Philpott MP. The human hair follicle engages in glutaminolysis and aerobic glycolysis: implications for skin, splanchnic and neoplastic metabolism. *Skin Pharmacol*. 1994;7:41-46.
22. Williams R, Philpott MP, Kealey T. Metabolism of freshly isolated human hair follicles capable of hair elongation: a glutaminolytic, aerobic glycolytic tissue. *J Invest Dermatol*. 1993;100:834-840.
23. Philpott MP, Kealey T. Metabolic studies on isolated hair follicles: hair follicles engage in aerobic glycolysis and do not demonstrate the glucose fatty acid cycle. *J Invest Dermatol*. 1991;96:875-879.
24. Hildyard JC, Ammala C, Dukes ID, et al. Identification and characterisation of a new class of highly specific and potent inhibitors of the mitochondrial pyruvate carrier. *Biochim Biophys Acta*. 2005;1707:221-230.
25. McNiff P, Svensson L, Pazoles CJ, et al. Tenidap modulates cytoplasmic pH and inhibits anion transport in vitro. I. Mechanism and evidence of functional significance. *J Immunol*. 1994;153:2180-2193.

26. Brailsford MA, Thompson AG, Kaderbhai N, et al. Pyruvate metabolism in castor-bean mitochondria. *Biochem J*. 1986;239:355-361.
27. Zhong Y, Li X, Yu D, et al. Application of mitochondrial pyruvate carrier blocker UK5099 creates metabolic reprogram and greater stem-like properties in LnCap prostate cancer cells in vitro. *Oncotarget*. 2015;6:37758-37769.
28. Patterson JN, Cousteils K, Lou JW, et al. Mitochondrial metabolism of pyruvate is essential for regulating glucose-stimulated insulin secretion. *J Biol Chem*. 2014;289:13335-13346.
29. Son MJ, Jeong JK, Kwon Y, et al. A novel and safe small molecule enhances hair follicle regeneration by facilitating metabolic reprogramming. *Exp Mol Med*. 2018;50:1-15.
30. Shin JM, Ko JW, Choi CW, et al. Deficiency of Crif1 in hair follicle stem cells retards hair growth cycle in adult mice. *PLoS ONE*. 2020;15:e0232206.
31. Yoon JS, Choi M, Shin CY, et al. Development of a model for chemotherapy-induced alopecia: profiling of histological changes in human hair follicles after chemotherapy. *J Invest Dermatol*. 2016;136:584-592.
32. Tellez-Segura R. Involvement of mechanical stress in androgenetic alopecia. *Int J Trichology*. 2015;7:95-99.
33. Arck PC, Handjiski B, Peters EM, et al. Topical minoxidil counteracts stress-induced hair growth inhibition in mice. *Exp Dermatol*. 2003;12:580-590.
34. Sundberg JP, King LE, Bascom C. Animal models for male pattern (androgenetic) alopecia. *Eur J Dermatol*. 2001;11:321-325.
35. Botchkarev VA, Komarova EA, Siebenhaar F, et al. p53 is essential for chemotherapy-induced hair loss. *Cancer Res*. 2000;60:5002-5006.
36. Uno H, Kurata S. Chemical agents and peptides affect hair growth. *J Invest Dermatol*. 1993;101:143S-147S.
37. Holland JM. Animal models of alopecia. *Clin Dermatol*. 1988;6:159-162.
38. Garza LA, Yang CC, Zhao T, et al. Bald scalp in men with androgenetic alopecia retains hair follicle stem cells but lacks CD200-rich and CD34-positive hair follicle progenitor cells. *J Clin Invest*. 2011;121:613-622.
39. Chen CC, Murray PJ, Jiang TX, et al. Regenerative hair waves in aging mice and extra-follicular modulators follistatin, dkk1, and sfrp4. *J Invest Dermatol*. 2014;134:2086-2096.
40. Reddy SK, Garza LA. The thinning top: why old people have less hair. *J Invest Dermatol*. 2014;134:2068-2069.
41. Giangreco A, Qin M, Pintar JE, et al. Epidermal stem cells are retained in vivo throughout skin aging. *Aging Cell*. 2008;7:250-259.
42. Liu N, Matsumura H, Kato T, et al. Stem cell competition orchestrates skin homeostasis and ageing. *Nature*. 2019;568:344-350.
43. Matsumura H, Mohri Y, Binh NT, et al. Hair follicle aging is driven by transepidermal elimination of stem cells via COL17A1 proteolysis. *Science*. 2016;351:aad4395.
44. Lavker RM, Zheng PS, Dong G. Morphology of aged skin. *Dermatol Clin*. 1986;4:379-389.
45. Tosti A, Piraccini BM, Vincenzi C, et al. Permanent alopecia after busulfan chemotherapy. *Br J Dermatol*. 2005;152:1056-1058.
46. Tran D, Sinclair RD, Schwarer AP, et al. Permanent alopecia following chemotherapy and bone marrow transplantation. *Australas J Dermatol*. 2000;41:106-108.
47. Ljungman P, Hassan M, Bekassy AN, et al. Busulfan concentration in relation to permanent alopecia in recipients of bone marrow transplants. *Bone Marrow Transplant*. 1995;15:869-871.
48. Parliament MB, Danjoux CE, Clayton T. Is cancer treatment toxicity accurately reported? *Int J Radiat Oncol Biol Phys*. 1985;11:603-608.
49. Paus R, Handjiski B, Eichmuller S, et al. Chemotherapy-induced alopecia in mice. Induction by cyclophosphamide, inhibition by cyclosporine A, and modulation by dexamethasone. *Am J Pathol*. 1994;144:719-734.
50. Hendrix S, Handjiski B, Peters EM, et al. A guide to assessing damage response pathways of the hair follicle: lessons from cyclophosphamide-induced alopecia in mice. *J Invest Dermatol*. 2005;125:42-51.
51. Kluger N, Jacot W, Frouin E, et al. Permanent scalp alopecia related to breast cancer chemotherapy by sequential fluorouracil/epirubicin/cyclophosphamide (FEC) and docetaxel: a prospective study of 20 patients. *Ann Oncol*. 2012;23:2879-2884.
52. Machado M, Moreb JS, Khan SA. Six cases of permanent alopecia after various conditioning regimens commonly used in hematopoietic stem cell transplantation. *Bone Marrow Transplant*. 2007;40:979-982.
53. Paus R, Haslam IS, Sharov AA, et al. Pathobiology of chemotherapy-induced hair loss. *Lancet Oncol*. 2013;14:e50-59.
54. Trueb RM. Chemotherapy-induced alopecia. *Semin Cutan Med Surg*. 2009;28:11-14.
55. Luznik L, Fuchs EJ. High-dose, post-transplantation cyclophosphamide to promote graft-host tolerance after allogeneic hematopoietic stem cell transplantation. *Immunol Res*. 2010;47:65-77.
56. Arck PC. Stress and pregnancy loss: role of immune mediators, hormones and neurotransmitters. *Am J Reprod Immunol*. 2001;46:117-123.
57. Arck PC, Handjiski B, Peters EM, et al. Stress inhibits hair growth in mice by induction of premature catagen development and deleterious perifollicular inflammatory events via neuropeptide substance P-dependent pathways. *Am J Pathol*. 2003;162:803-814.
58. Ito N, Ito T, Kromminga A, et al. Human hair follicles display a functional equivalent of the hypothalamic-pituitary-adrenal axis and synthesize cortisol. *FASEB J*. 2005;19:1332-1334.
59. Foitzik K, Krause K, Nixon AJ, et al. Prolactin and its receptor are expressed in murine hair follicle epithelium, show hair cycle-dependent expression, and induce catagen. *Am J Pathol*. 2003;162:1611-1621.
60. Grahovac T, Ruzic K, Sepic-Grahovac D, et al. Depressive disorder and alopecia. *Psychiatr Danub*. 2010;22:293-295.
61. Van Neste D, Tobin DJ. Hair cycle and hair pigmentation: dynamic interactions and changes associated with aging. *Micron*. 2004;35:193-200.
62. Brajac I, Tkalcic M, Dragojevic DM, et al. Roles of stress, stress perception and trait-anxiety in the onset and course of alopecia areata. *J Dermatol*. 2003;30:871-878.
63. Rebora A. Telogen effluvium. *Dermatology*. 1997;195:209-212.
64. Heidt T, Sager HB, Courties G, et al. Chronic variable stress activates hematopoietic stem cells. *Nat Med*. 2014;20:754-758.
65. Zang B, Ma S, Rachmin I, et al. Hyperactivation of sympathetic nerves drives depletion of melanocyte stem cells. *Nature*. 2020;577(7792):676-681.
66. Plikus MV, Mayer JA, de la Cruz D, et al. Cyclic dermal BMP signalling regulates stem cell activation during hair regeneration. *Nature*. 2008;451:340-344.

SUPPORTING INFORMATION

Additional supporting information may be found online in the Supporting Information section.

App S1. Materials and Methods.

How to cite this article: Flores A, Choi S, Hsu Y-C, Lowry WE. Inhibition of pyruvate oxidation as a versatile stimulator of the hair cycle in models of alopecia. *Exp Dermatol*. 2021;30:448–456. https://doi.org/10.1111/exd.14307

Materials and Methods

Animal experiments

All animal experiments and related procedures were performed in accordance with protocols approved by the Institutional Animal Care and Use Committee (IACUC) at UCLA in facilities overseen by the UCLA Department of Laboratory Animal Medicine (DLAM). Male wildtype C57BL/6J animals were obtained from The Jackson Laboratory (Stock No: 000664). No statistical measure was used to determine the sample size beforehand. The results described include data from all treated animals. The investigators were not blinded to allocation during the experimental data collection, nor were the experiments randomized. The results shown are representative images from at least three independently treated animals per condition as denoted in each experimental legend.

Age-induced Alopecia

Aged male C57BL/6J mice were obtained from Jackson Laboratories at 78 weeks old (Stock No:000664). Upon arrival, mice showed thinning and greying hair. Mice were shaved and observed for hair regrowth. This was repeated three times until the hair no longer grew back to full coverage. Mice were 87 weeks at start of topical treatment. Mice were treated topically with either Transderma Plo gel (Vehicle) or 20uM UK5099 in Vehicle every other day for 30 days. 200ul of lotion was applied evenly to the backskin of mice using a cotton swab. Macroscopic observations were made, and at the end of 30 days, tissue was harvested, embedded in OCT, sectioned and histology performed. Immunofluorescence staining was performed with the following antibodies: Ki67 (Abcam ab16667, 1:50), Sox9 (Abcam ab185230, 1:1000).

Chemotherapy induced Alopecia

Male and female C57BL/6 mice (Stock No: 000664) were obtained from Jackson Laboratories at 7 weeks of age. Hair growth was induced by depilating the hairs with a wax/rosin mixture (Nads Body Wax Strips). At day 9 after depilation, when all follicles are in anagen VI, 120 mg per kg body weight cyclophosphamide was injected intraperitoneally. Complete hair loss from the backskin was observed within a week. Following this, mice were observed for regrowth of hair and full hair coverage was achieved within 2-3 weeks. Depilation and cyclophosphamide treatment was repeated 7 more times until the hair no longer grew back completely. Mice were then treated topically with either Transderma Plo gel (Vehicle) or 20uM UK5099 in Vehicle every other day for 30 days. 200ul of lotion was applied evenly to the backskin of mice using a cotton swab. Macroscopic observations were made, and at the end of 30 days, tissue was harvested, embedded in OCT, sectioned and histology performed. Immunofluorescence staining was performed with the following antibodies: Ki67 (Abcam ab16667, 1:50), Sox9 (Abcam ab185230, 1:1000).

Alopecia due to chronic stress

Mice were subjected to various noxious stimuli as described in (Heidt et. al.) (64), until hair did not grow back for an extended period. Mice were then treated topically with either Transderma Plo gel (Vehicle) or 20uM UK5099 in Vehicle every other day for 30 days. 200ul of lotion was applied evenly to the backskin of mice using a cotton swab. As a control, wildtype mice not exposed to stressful stimuli were also treated with Vehicle or 20uM UK5099. Macroscopic observations were made, and at the end of 30 days, tissue was harvested, embedded in OCT, sectioned and histology performed. Immunofluorescence staining was performed with the following antibodies: Ki67 (Abcam ab16667, 1:50), Sox9 (Abcam ab185230, 1:1000).

Histology and Immunostaining

At the completion of each experiment, treated dorsal back skins of mice were harvested and embedded in OCT compound for frozen tissue preparations, or fixed overnight in 4% formalin and embedded in paraffin. For frozen tissue, 10 μm sections were cut with a Leica 3200 Cryostat, fixed for 5 minutes in 4% paraformaldehyde and stained with hematoxylin and eosin (Vector Laboratories, H-3502). For immunofluorescence staining, frozen sections were fixed and blocked in staining buffer containing appropriate control IgG (goat, rabbit etc.) with the following antibodies: Ki67 (Abcam ab16667, 1:50), Sox9 (Abcam ab185230, 1:1000. Images were taken on an Olympus BX43 Upright Microscope and Zeiss Model Axio Imager M1 Upright Fluorescence Microscope.

Statistics and reproducibility

Experiments were performed on male animals and all phenotypes described are representative of a minimum of n = 6 littermate pairs (or a total of twelve mice) as indicated in the description of each experiment. For analysis of the hair regrowth phenotype, no statistical measure was used to determine the sample size beforehand, nor were statistics used to measure effects, as the results were essentially positive or negative as represented in the figures. The results described include data from all treated animals. Investigators were not blinded to allocation during the experimental data collection. Experiments were not randomized. All results shown are representative images from at least three independently treated animals, and genotyping was performed both before and after animal treatment for confirmation. Pairwise comparisons between two groups were performed by two-tailed statistical analysis using Student's t test. Statistical significances were considered if $*p < 0.05$; $**p < 0.01$; $***p < 0.001$. Experimental data

are demonstrated as the mean ± SEM. Sample size and statistical details can be found in the figure legends.